

Allele-specific silencing as treatment for gene duplication disorders: proof-of-principle in autosomal dominant leukodystrophy

Elisa Giorgio,¹ Martina Lorenzati,² Pia Rivetti di Val Cervo,³ Alessandro Brussino,¹ Manuel Cernigoj,³ Edoardo Della Sala,¹ Anna Bartoletti Stella,⁴ Marta Ferrero,¹ Massimiliano Caiazzo,^{5,6} Sabina Capellari,^{4,7} Pietro Cortelli,^{4,7} Luciano Conti,⁸ Elena Cattaneo,^{3,9} Annalisa Buffo² and Alfredo Brusco^{1,10}

Allele-specific silencing by RNA interference (ASP-siRNA) holds promise as a therapeutic strategy for downregulating a single mutant allele with minimal suppression of the corresponding wild-type allele. This approach has been effectively used to target autosomal dominant mutations and single nucleotide polymorphisms linked with aberrantly expanded trinucleotide repeats. Here, we propose ASP-siRNA as a preferable choice to target duplicated disease genes, avoiding potentially harmful excessive downregulation. As a proof-of-concept, we studied autosomal dominant adult-onset demyelinating leukodystrophy (ADLD) due to lamin B1 (*LMNB1*) duplication, a hereditary, progressive and fatal disorder affecting myelin in the CNS. Using a reporter system, we screened the most efficient ASP-siRNAs preferentially targeting one of the alleles at rs1051644 (average minor allele frequency: 0.45) located in the 3' untranslated region of the gene. We identified four siRNAs with a high efficacy and allele-specificity, which were tested in ADLD patient-derived fibroblasts. Three of the small interfering RNAs were highly selective for the target allele and restored both *LMNB1* mRNA and protein levels close to control levels. Furthermore, small interfering RNA treatment abrogates the ADLD-specific phenotypes in fibroblasts and in two disease-relevant cellular models: murine oligodendrocytes overexpressing human *LMNB1*, and neurons directly reprogrammed from patients' fibroblasts. In conclusion, we demonstrated that ASP-silencing by RNA interference is a suitable and promising therapeutic option for ADLD. Moreover, our results have a broad translational value extending to several pathological conditions linked to gene-gain in copy number variations.

- 1 University of Torino, Department of Medical Sciences, 10126, Torino, Italy
- 2 University of Torino, Department of Neuroscience Rita Levi Montalcini and Neuroscience Institute Cavalieri Ottolenghi (NICO), Orbassano, 10043, Torino, Italy
- 3 University of Milan, Department of Biosciences, Laboratory of Stem Cell Biology and Pharmacology of Neurodegenerative Diseases, 20122 Milan, Italy
- 4 IRCCS Istituto delle Scienze Neurologiche di Bologna, Bellaria Hospital, 40139, Bologna, Italy
- 5 Department of Pharmaceutics, Utrecht Institute for Pharmaceutical Sciences (UIPS), Utrecht University, Universiteitsweg 99, 3584, CG, Utrecht, The Netherlands
- 6 Department of Molecular Medicine and Medical Biotechnology, University of Naples 'Federico II', 80131, Naples, Italy
- 7 University of Bologna, Department of Biomedical and Neuromotor Sciences, 40123, Bologna, Italy
- 8 University of Trento, Centre for Integrative Biology (CIBIO), Laboratory of Computational Oncology, 38123, Trento, Italy
- 9 National Institute of Molecular Genetics (INGM) Romeo and Enrica Invernizzi, 20122, Milano, Italy
- 10 Città della Salute e della Scienza University Hospital, Medical Genetics Unit, 10126, Torino, Italy

Correspondence to: Alfredo Brusco

University of Torino, Department of Medical Sciences, via Santena 19, 10126, Torino, Italy

E-mail: alfredo.brusco@unito.it

Keywords: ADLD; LMNB1; leukodystrophy; RNA therapeutics; siRNA

Abbreviations: ADLD = autosomal dominant adult-onset demyelinating leukodystrophy; ASP-RNAi = allele-specific silencing by RNA interference; OPC = oligodendrocyte precursor cell; SNP = single nucleotide polymorphism

Introduction

Autosomal dominant adult-onset demyelinating leukodystrophy (ADLD, OMIM#169500) (Eldridge *et al.*, 1984) is a slowly progressive disease which occurs in the fourth to fifth decade of life with autonomic symptoms, which can precede cerebellar and pyramidal abnormalities by several years. Loss of fine motor control and gait disturbance appear later and culminate in slowly progressive spastic tetraparesis, ataxia, and incontinence (Quattrocchio *et al.*, 1997; Coffeen *et al.*, 2000; Nahhas, 2016). Only symptomatic and palliative treatments are presently available. ADLD is caused by excessive LMNB1 production due to gene duplication (Padiath *et al.*, 2006; Giorgio *et al.*, 2013) or to alteration of the LMNB1 regulatory landscape (Giorgio *et al.*, 2015; Nmezi *et al.*, 2019).

At the cellular level, LMNB1 regulates nuclear mechanics and integrity (Ferrera *et al.*, 2014), interacts with chromatin determining chromosome segregation (Guelen *et al.*, 2008), and regulates gene expression through mRNA synthesis (Tang *et al.*, 2008) and splicing (Camps *et al.*, 2014; Bartoletti-Stella *et al.*, 2015). The pathogenic mechanisms underlying ADLD have only begun to be explored and directly involve LMNB1 overexpression (Heng *et al.*, 2013; Bartoletti-Stella *et al.*, 2015; Rolyan *et al.*, 2015; Giacomini *et al.*, 2016). It stands to reason that genetic modulation of LMNB1 mRNA/protein represents a promising strategy for treating ADLD (Lin and Fu, 2009).

In recent years, the use of synthetic small interfering RNAs (siRNAs) has become a popular choice for the development of gene-silencing based therapies (Bumcrot *et al.*, 2006; Dykxhoorn and Lieberman, 2006; Levin, 2019). A handful of siRNAs have recently entered clinical trials, and others are clinically approved or in preclinical development for diseases such as autosomal dominant transthyretin amyloidosis, respiratory syncytial virus infection, solid tumours, age-related macular degeneration, diabetic macular oedema, congenital pachyonychia, and haemophilia (Dykxhoorn and Lieberman, 2006; de Fougères *et al.*, 2007; Haussecker, 2008; Nguyen *et al.*, 2008; Smith *et al.*, 2008; Whitehead *et al.*, 2009; Davis *et al.*, 2010; DeVincenzo *et al.*, 2010; Coelho *et al.*, 2013) (see clinicaltrials.gov).

However, a major drawback is dysregulation and excessive transcript reduction of the target, which may lead to pathogenic consequences. This concern is due to the fact that dosage-sensitive genes often cause pathological phenotypes either in excess or deficit (Antonarakis, 2017; Deshpande and Weiss, 2018). Two instructive examples are the 16p11.2-related microcephaly/macrocephaly caused by duplications or deletions encompassing the

KCTD13 gene (Jacquemont *et al.*, 2011), and Charcot-Marie-Tooth disease type 1A (CMT1A)/hereditary neuropathy with liability to pressure palsies (HNPP), associated with peripheral myelin protein 22 (*PMP22*) duplication or deletion, respectively (van Paassen *et al.*, 2014).

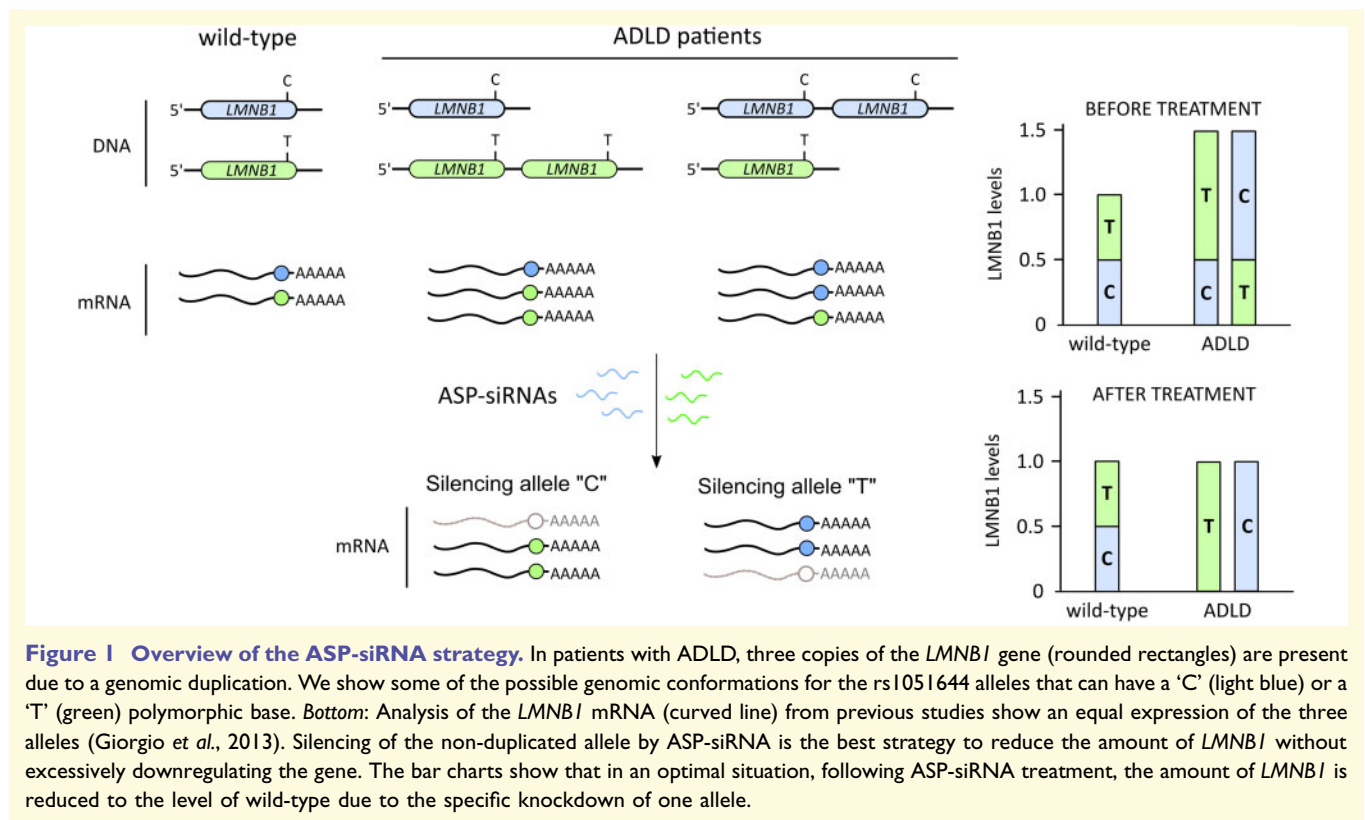
Other than a complete suppression of the target gene, allele-specific silencing by RNA interference (ASP-RNAi) has been proposed as a variant gene-silencing strategy that allows downregulation of the mutant allele with minimal suppression of the corresponding wild-type allele. ASP-RNAi has been used to target gain-of-function autosomal dominant mutations (Miller *et al.*, 2004; Liao *et al.*, 2011; Loy *et al.*, 2012; Takahashi *et al.*, 2012; Allen *et al.*, 2013) and single nucleotide polymorphisms (SNPs) in *cis* with an aberrant transcript, such as in diseases with expanded polyglutamine encoding CAG-repeats [spinocerebellar ataxia (SCA) 1, SCA3, SCA7, and Huntington's disease] (Miller *et al.*, 2003; Alves *et al.*, 2008; Scholefield *et al.*, 2009; Takahashi *et al.*, 2010; Nobrega *et al.*, 2013, 2014). It stands to reason that gene-silencing approaches represent the main therapeutic strategy also for genetic diseases associated with gene duplication.

In this study, we investigated the therapeutic potential of ASP-RNAi for gene duplication disorders, demonstrating a proof-of-principle in ADLD.

Compared to other antisense strategies, this approach allows avoiding potentially harmful excessive downregulation of the target gene. This latter point seems to be relevant for *LMNB1*, where excessive silencing may have deleterious effects, as shown in cellular and mouse models (Liu *et al.*, 2000; Harborth *et al.*, 2001; Vergnes *et al.*, 2004; Ji *et al.*, 2007; Coffinier *et al.*, 2010, 2011; Bartoletti-Stella *et al.*, 2015; Giacomini *et al.*, 2016).

Since ADLD patients have three equally-expressed *LMNB1* alleles (Giorgio *et al.*, 2013), we chose to target the non-duplicated allele of the *LMNB1* gene by ASP-siRNAs, with the aim of reducing expression close to wild-type levels (Fig. 1). To discriminate the three *LMNB1* alleles in ADLD patients, we exploited the SNP rs1051644, located in the 3' untranslated region (UTR) of the gene. This polymorphism has an allele frequency ranging from 0.3 (African), 0.46 (European) to 0.53 (East Asian) (<http://gnomad.broadinstitute.org>) (Lek *et al.*, 2016); among our 10 patients with ADLD, eight carried one allele (non-duplicated allele) different from the other two (duplicated allele) (possible genotypes: C-C-T or T-T-C).

To the best of our knowledge, this is the first application of an ASP-RNAi strategy to diseases caused by gene duplications, opening new therapeutic opportunities for



several pathological conditions linked to gene copy number gains.

Materials and methods

Plasmid vectors are described in the Supplementary material.

Cell lines and cell culture

Fibroblast cell lines were obtained from four ADLD patients (Patients IT1, IT2, IT3, and BR1; see Giorgio *et al.*, 2013) and three age-matched control subjects. Patients IT1, IT2, and IT3 carry the 'C' allele of the targeted SNP on the duplicated *LMNB1* copy (hereafter named 'dupC'), whereas in Patient BR1 the 'T' allele is duplicated (hereafter named 'dupT').

The HEK293T cells and patients' derived fibroblasts were cultured in Dulbecco's modified Eagle's medium (DMEM; Thermo Fisher Scientific) with the addition of 10% foetal bovine serum (FBS; Thermo Fisher Scientific). All cultures were incubated at 37°C in the presence of 5% CO₂. For direct-reprogramming experiments, human primary fibroblasts from healthy and ADLD donors were cultured in DMEM supplemented with 10% FBS, 0.5% Pen-Strep, 2 mM glutamine, 1 mM sodium pyruvate and 1% non-essential amino acids (Thermo Fisher Scientific).

Primary oligodendrocyte precursor cells (OPCs) were isolated by shaking method from mixed glial cultures obtained from postnatal Day 0–2 Sprague-Dawley rat cortex, as described in Boda *et al.* (2015). OPCs were plated at 20 000 cells/cm² onto poly-D-lysine (1 mg/ml, Sigma-Aldrich) coated

Thermo Scientific Nunc Lab-Tek II chambered coverglass, and cultured in Neurobasal™ with 1X B27 (Invitrogen), 2 mM L-glutamine, 10 ng/ml human platelet derived growth factor (PDGF)-BB and 10 ng/ml human basic fibroblast growth factor (bFGF) (Miltenyi Biotec).

Design of siRNAs and generation of shRNA recombinant lentivirus particles

We designed an siRNA library with a 19+2 bp geometry, as described in Schwarz *et al.* (2006), targeting the 'C' or the 'T' alleles of the rs1051644 SNP. Because bioinformatics cannot optimally predict the best allele-specific siRNAs, all 19 possible siRNAs were considered (Supplementary Table 2). An siRNA targeting the *Renilla luciferase* gene (siRen, C+) and a non-specific siRNA (scramble) were used as controls in the experiments. All siRNAs were synthesized with a dTdT 3'-end tail by Eurofins Genomics.

The most efficient ASP-siRNA (SNP position 4) targeting the T allele was converted to generate a mCherry-tagged short-hairpin RNA expression vector and cloned into recombinant lentivirus particles (LV-ASP-T4 shRNA; pLV[shRNA]-mCherry:T2A:Puro-U6; viral titre 1.62 × 10⁹ TU/ml; outsourced to VectorBuilder). As negative control, we used a commercial GFP-tagged scramble shRNA control lentivirus (scramble shRNA; viral titre 9.59 × 10⁸ TU/ml, VB151023–10034; Vector Builder; LV–). The lentiviral particles produced were resuspended in Hank's balanced salt solution buffer. Viral stocks were stored at –80°C until use. Virus was subsequently titred in primary cultures of rat OPCs (see below) by

serial dilutions. Five days post-infection, cells were collected, and the rate of transduction evaluated by fluorescent microscopy.

Dual luciferase reporter assay

HEK293T cells were seeded at a concentration of 2.5×10^4 cells/well in a 96-well plate and incubated for 24 h in DMEM supplemented with 5% foetal calf serum (FCS) without antibiotics. Twenty nanograms of the psiCHEK-LMNB1-3'UTR-C or the psiCHEK-LMNB1-3'UTR-T vectors were co-transfected with each of the siRNAs at two different concentrations (12.5 nM or 30 nM) using LipofectamineTM 2000, following the manufacturer's protocol (Thermo Fisher Scientific). Chemiluminescence was measured at 48 h post-transfection using the Dual-Luciferase[®] Reporter Assay System (Promega) on an analytical GloMax[®] 20/20 luminometer (Promega). All 19 SNP-specific siRNAs, as well as siRen and scramble siRNA were tested, evaluating their ability to silence the targeted psiCHEK-LMNB1-3'UTR plasmid. For each assay, we performed at least three independent technical replicas.

Validation of allele-specific siRNAs in ADLD fibroblasts

ADLD and control fibroblasts were seeded at a concentration of 1.5×10^5 cells/well in a 6-well plate and incubated for 24 h in DMEM supplemented with 5% FCS without antibiotics. Cells were transfected with allele-specific siRNAs, a non-allele-specific *LMNB1* siRNA (C+) and a scramble siRNA (AM 4620, Thermo Fisher Scientific) at two concentrations (40 nM and 100 nM) using LipofectamineTM 2000 (Thermo Fisher Scientific). Cells were harvested at 48 h post transfection and split to extract RNA and proteins.

To evaluate the ability of siRNAs to rescue ADLD-specific cellular phenotypes, ADLD and control fibroblasts were transfected using LipofectamineTM 2000 (Thermo Fisher Scientific) at T0 and T72 h with 100 nM of the allele-specific siRNAs, a non-allele-specific *LMNB1* siRNA (C+) and a scramble siRNA (AM 4620, Thermo Fisher Scientific). Since the rescue of the reported cellular phenotypes is subsequent to *LMNB1* modulation, we harvested cells at 120 h post transfection. For each siRNA, at least three independent experiments were performed. Because of technical reasons, we were not able to test ASP-siRNA in cells from Patient BR1.

Direct reprogramming of ADLD and control human fibroblasts in neurons

Viral production and titration

HEK293NT cells were plated on gelatin coated dishes at a density of 45 000 cells/cm², and were transfected on the following day with LipofectamineTM 3000 according to the manufacturer's instructions for the production of LV-ABR (L3000015, Thermo Fisher Scientific). The LV-ABR plasmid was co-transfected with the third generation packaging vectors pMDLg/pRRE (Addgene 12251), pRSV-Rev (Addgene 12253), and pMd2.G (Addgene 12259) in a 4:2:1:1 ratio. The transfection mix was removed after an overnight incubation, and fresh media was supplied to the cells. The supernatant was

collected 48 h and 72 h post-transfection and centrifuged at 60 000g for 2 h; the concentrated viral particles were resuspended in phosphate-buffered saline (PBS) buffer overnight.

The virus was subsequently titred in MRC5 human fibroblasts in a serial dilution. Seventy-two hours post-infection cells were collected, the DNA extracted and the number of integrated proviruses/ml was measured by real-time quantitative PCR and compared to a standard curve with primers listed in Supplementary Table 1.

Direct neuronal reprogramming

Low-passage primary human fibroblasts (<P6) from healthy donors ($n = 3$) and ADLD patients [$n = 3$; IT1, IT2 and IT3, (Giorgio *et al.*, 2013)] were plated on poly-L-ornithine-Laminin-Fibronectin (Shrigley *et al.*, 2018) coated optical plate (96 well micro-plates, #89626, Ibbidi), at a density of 10 000 cells/cm² (Drouin-Ouellet *et al.*, 2017b). The next day (reprogramming Day 0, d0), cells were infected with lentiviral particles in the presence of polybrene 4 µg/ml overnight with LV-ABR at a multiplicity of infection (MOI) of 20. On the following day fresh fibroblasts medium substituted the infection medium, and 48 h later the fibroblasts medium was changed to reprogramming medium from Day 2 to 18 (half medium change); from Day 18 the medium was switched to maturation medium (Drouin-Ouellet *et al.*, 2017b).

Validation of allele-specific shRNAs in ADLD neurons

Cells were transduced with lentiviral particles (LV-ASP-T4 shRNA or LV-scramble shRNA) at a MOI of 50/80. We tested two different experimental protocols: (i) fibroblasts were transduced with lentiviral particles at reprogramming Day 0 (MOI 50, transduction efficiency of ~75%); and (ii) fibroblasts were reprogrammed into neurons, and at Day 13 of reprogramming (d13) were transduced with lentivirus (MOI 80, transduction efficiency comparable to Day 0). At Day 20, cells were fixed in paraformaldehyde (PFA) 4% for 15 min at 4°C for immunocytochemistry. To evaluate the effect of LV-ASP-T4 shRNA, we performed *LMNB1* expression analysis and immunofluorescence evaluations of *LMNB1* protein level, nuclear alterations and neurite features (see below).

Validation of allele-specific shRNAs in rat oligodendrocytes cultures overexpressing human *LMNB1* coding sequence

After the shaking procedure, on the first day after plating, part of the cells was transduced with lentiviral particles (LV-ASP-T4 shRNA) at a MOI of 50, that yielded a transduction efficiency of ~60%. The rest of the cells were used as mock controls to define mouse *LMNB1* levels. Five days later, transduced cells were transfected with human (h)*LMNB1*-GFP (allele 'T' or 'C') construct or a CAGP-AcGFP1 (GFP) empty vector using LipofectamineTM 2000 (Thermo Fisher Scientific), following the manufacturer's protocol. Cells were harvested 48 h post transfection, fixed for 20 min in 4% PFA in 0.1 M phosphate buffer and processed for immunohistochemistry to analyse *LMNB1* levels and nuclear alterations.

RNA isolation and quantitative real time PCR

Total RNA was extracted from fibroblasts using the Direct-Zol RNA MiniPrep system (Zymo Research) and cDNA was generated using the M-MLV Reverse Transcriptase kit (Invitrogen). The expression levels of *LMNB1*, ribonucleoprotein, PTB binding 2 (*RAVER2*), leucine rich repeat containing 15 (*LRRCL5*) and the reference gene hydroxymethylbilane synthase (*HMBS*) were measured with predesigned TaqMan™ assays (Applied Biosystems, *LMNB1*, Hs01059210_m1; *RAVER2*, Hs00217122_m1; *LRRCL5*, Hs00370056_s1; *HMBS*, Hs00609297_m1).

Reactions were carried out in triplicate on an ABI 7500 real-time PCR machine using the ABI 2X TaqMan™ Universal PCR Master Mix II, according to the manufacturer's instructions (Thermo Fisher Scientific).

Allelic discrimination by primer extension assay

To evaluate the relative amount of the two *LMNB1* alleles after ASP-siRNA treatment, we used an in-house developed primer extension assay based on the SNaPshot® System (Thermo Fisher Scientific) (Giorgio *et al.*, 2013). In brief, we extracted total RNA, retrotranscribed cDNA, and amplified a 394-bp region of the *LMNB1* 3'-UTR. After primer extension, reactions were purified using shrimp alkaline phosphatase (SAP, Fermentas), loaded on an ABI-Prism 3730xl DNA analyser with a GS120-Liz marker, and analysed using the GeneScan ver 3.7 software (Applied Biosystems, Thermo Fisher Scientific). Using peak height, we calculate the fraction of each allele using the formula: allele 'C' = $[C / (C + T)]$; allele 'T' = $[T / (C + T)]$.

Western blot analysis

Total protein was extracted from fibroblasts in RIPA buffer. Seven micrograms of protein extracts were run on NuPAGE 4–12% Bis-Tris Gel (Invitrogen, Thermo Fisher Scientific), then blotted onto nitrocellulose (Bio-Rad) in Tris/glycine buffer with 20% methanol at 4°C for 90 min. Protein transfer efficiency was evaluated using the MemCode Reversible Protein Stain Kit (Pierce Biotechnology). *LMNB1* and beta-actin were detected using primary anti-lamin B1 (ab16048, Abcam) and anti-beta actin (ab8227, Abcam) antibodies and WesternBreeze™ Chemiluminescent Detection Kit (Invitrogen, Thermo Fisher Scientific). Images were captured with a ChemiDoc™ XRS+ System and densitometry analysis was performed with Image Lab™ Software (Bio-Rad).

Immunofluorescence

Fibroblasts

Cells were plated onto coverslips, transfected/transduced with siRNAs/LV-shRNAs as described previously, fixed in 4% PFA and immunolabelled as described previously (Giorgio *et al.*, 2015). Samples were immunostained using rabbit polyclonal anti-*LMNB1* (ab16048, Abcam) and Alexa Fluor® 488 goat anti-rabbit secondary antibody (Thermo Fisher

Scientific). The confocal optical sectioning was performed at room temperature using a Leica TCS SP5 AOBS TANDEM inverted confocal microscope that was equipped with a 40 × HCX PL APO 1.25 oil objective lens. For each experimental point, at least 90 nuclei were analysed. Three technical replicates were performed. A total of 5391 nuclei were analysed blindly.

Reprogrammed neurons and primary oligodendrocyte precursors cell cultures

Reprogrammed neurons and primary OPC cultures were processed according to standard immunocytochemical procedures (Boda *et al.*, 2015). Cells were immunostained with polyclonal rabbit anti-*LMNB1* (1:2000, as above), mouse monoclonal anti-β-III tubulin (1:800, Promega), or rabbit polyclonal NG2 antiserum (1:400, Millipore). Secondary antibodies were Cy3- (Jackson ImmunoResearch Laboratories), Alexa Fluor® 488-, and Alexa Fluor® 647-conjugated (Molecular Probes Inc.). All antibodies were diluted in a phosphate buffer blocking solution containing 0.3% Triton™ X-100. To counterstain cell nuclei, we used 4,6-diamidino-2-phenylindole (DAPI, Fluka) or TO-PRO®-3 stain (Thermo Fisher Scientific).

In a set-up experiment, we analysed reprogrammed neurons in one healthy donor and one patient (Patient IT2) to evaluate recombination efficiency (Supplementary Fig. 1), and define primary *LMNB1* protein overexpression) and secondary (nuclear alterations) pathological readouts in patients' cells (Supplementary Fig. 1). To this aim, 200–300 cells in two technical replicates were examined for a total of ~600 cells. In the main experiments, we used three healthy donors and three patients with ADLD in two biological replicates (see above). About 600 neuronal nuclei for each experimental point were evaluated by densitometric analysis for a total of ~6700 cells. Two independent experiments with three technical replicates were performed. Images including stacks of the whole cells were acquired with a Leica TCS SP8 confocal microscope and analysed with NIH ImageJ software to obtain *LMNB1* protein immunofluorescent signal intensity. The nuclear outline was drawn on confocal images based on DAPI or TO-PRO®-3 signals, and the integrated density measure of *LMNB1* protein content was obtained. Reprogrammed neurons were distinguished from fibroblasts based on morphological criteria (size and shape of the nucleus, elongated morphology and presence of processes), as validated by anti-β-III tubulin staining (Supplementary Fig. 1). For nuclear alterations, *LMNB1* protein appearance in reprogrammed neurons was classified as follows: homogeneous, forming stripes, forming crumples (Supplementary Fig. 1). For evaluation of neurite growth, for each field of view (pictures obtained at ×40 magnification) we quantified the number of neurite intersections on a superimposed grid (area of 500 μm²) and normalized this number by the number of neuronal somata in the corresponding field.

Note that because of the different reporter of sh*LMNB1* and scramble viral particles, distinct sets of reprogrammed neurons were stained for *LMNB1* protein with different fluorophores (green Alexa Fluor® 466, or red Cy3) to assess variations in *LMNB1* protein levels. After confirming no significant changes between detected levels of *LMNB1* in ADLD and control mock conditions with both the two immunostaining procedures ($P = 0.4690$), each value for each experimental condition was

normalized over the colour-matched mock average value. The normalized values were used to compare scramble versus shLMNB1 samples in statistical analyses.

Upon transfection with hLMNB1-GFP, we analysed OPC cultures as indicated above to define primary (LMNB1 over-expression) and secondary (nuclear alterations) pathological readouts (Supplementary Fig. 2). About 3300 cells were inspected (two experiments; three technical replicates) and we obtained a transfection efficiency (GFP-positive cells) of about 3%. To examine silencing efficiency, we performed two independent sets of experiments each with three technical replicates analysing a total of ~2500 cells per round. We performed densitometric analyses of LMNB1 protein using either anti-LMNB1 protein immunofluorescent staining or GFP-tag signal.

Statistical analysis

Graphics and statistical analysis were performed with Graphpad Prism version 5.00 (Graphpad software, San Diego, CA). Data are presented as mean \pm standard error of the mean (SEM). All data were analysed using two-tailed Mann-Whitney *t*-test. For immunofluorescence experiments, statistical analyses were performed using the mean values for each analysed field as samples. Values are calculated relative to scramble siRNA/shRNA using average of at least two independent experiments.

Data availability

The authors confirm that the data supporting the findings of this study are available within the Supplementary material.

Results

Identification of allele-specific siRNAs

To exploit the ASP-RNAi strategy, we searched for a frequent SNP within the *LMNB1* transcribed region. We found only four SNPs with a minor allele frequency (MAF) $>5\%$ in the dbSNP142 (rs35091677, MAF 0.357 ± 0.226 ; rs6875053, 0.068 ± 0.171 ; rs1051643, 0.440 ± 0.162 ; rs1051644, 0.495 ± 0.052). Among these, we chose to target the SNP with the highest MAF, rs1051644, which mapped to the *LMNB1* 3'-UTR. Because the three *LMNB1* alleles in patients with ADLD are equally expressed (Giorgio *et al.*, 2013), targeting the non-duplicated allele of the *LMNB1* was expected to reduce expression close to wild-type (see rationale in Fig. 1).

Bioinformatics tools that evaluate siRNA efficiency are poor at predicting allele specificity (Hohjoh, 2013). Thus, we designed a strategy to screen for siRNAs with the highest capacity for efficient and selective silencing of one allele of the rs1051644 SNP (rationale summarized in Fig. 2A). We used a dual reporter plasmid, containing the Firefly luciferase gene fused to part of the *LMNB1* 3'-UTR and the *Renilla* luciferase gene, to test all

the 19 possible siRNAs (19 + 2 bp geometry) that targeted the 'C' or the 'T' allele of rs1051644 (Supplementary Table 2).

The results are summarized in Fig. 2B and C. We identified three non-efficient siRNAs ($<70\%$ reduction of the target allele at 30 nM; SNP positions 2, 8, and 13) and 16 efficient siRNAs (SNP positions 1, 3–7, 9–12, and 14–19). Only five of these showed statistically different allele specificity, at both concentrations tested (Fig. 2B and C; SNP positions 3–6, and 9). Based on ASP-siRNA definition (Allen *et al.*, 2013), we further selected siRNAs 3–5, and 9, which strongly knocked down the target allele at the lower concentration tested while minimally affecting the non-target allele at the highest concentration tested (Supplementary Table 3).

ASP-siRNAs restored physiological LMNB1 levels and ameliorated ADLD cellular phenotypes in patient fibroblasts

Human ADLD fibroblasts represent a genetically accurate model to assess siRNA allele specificity (Scholefield *et al.*, 2014). These fibroblasts have the genomic context with *LMNB1* duplication, are easy to manipulate, and allow the readout for ADLD-associated phenotypes, such as nuclear blebs and altered gene expression (Ferrera *et al.*, 2014; Bartoletti-Stella *et al.*, 2015; Giorgio *et al.*, 2015).

We evaluated the efficiency of selected siRNAs by measuring *LMNB1* versus *HMBS* (reference gene) by RT-qPCR in ADLD fibroblasts (Fig. 3A). We observed that ASP-siRNAs 3–5 and 9 significantly reduced *LMNB1* mRNA levels both at 40 nM (Supplementary Table 4) and 100 nM (Fig. 3A and Supplementary Table 4). Interestingly, three ASP-siRNAs (3, 4, and 9 at 100 nM) restored *LMNB1* expression to physiological levels. At the same concentrations (40 nM and 100 nM), the non-allele specific siRNA (*LMNB1* CTRL+) reduced *LMNB1* expression close to zero (Supplementary Table 4).

We accurately evaluated allele specificity of these four selected siRNAs exploiting a primer extension assay previously developed by our group (Giorgio *et al.*, 2013) (Fig. 3B). ASP-siRNAs T3, T4 and T9 preferentially silenced the matched 'T' allele, at both tested concentrations. On the other hand, only C3 and C4 siRNAs showed significant allele specificity for the matched *LMNB1* allele (Fig. 3B and Supplementary Table 5). Both siRNAs with the SNP at position 5 did not show statistically significant allele specificity (T5 and C5 in Fig. 3B and Supplementary Table 5). Overall, these results demonstrated the efficiency and allele specificity of T3, T4, T9, C3 and C4 siRNAs.

Next, we verified if the reduction in *LMNB1* mRNA correlated with decreased protein. All ASP-siRNAs (SNP

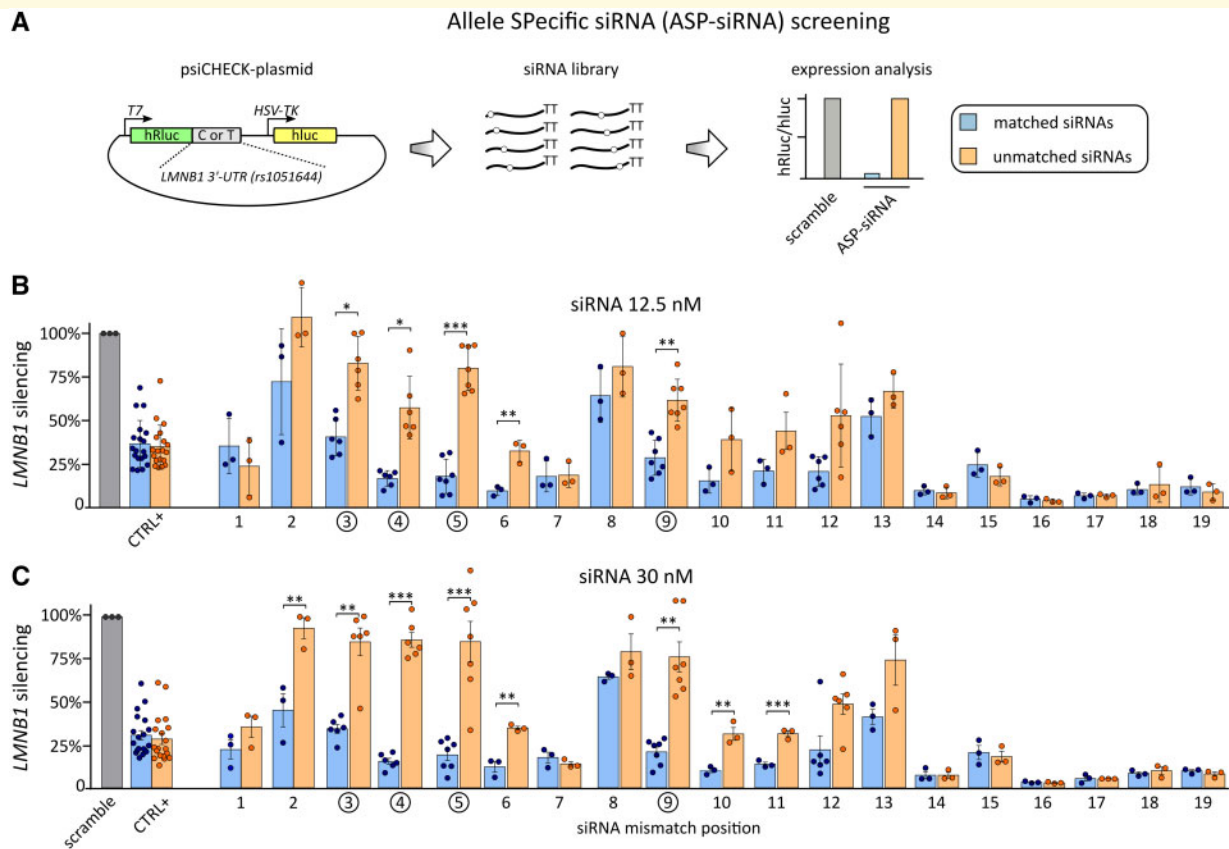


Figure 2 ASP-siRNA screening. (A) The rationale used to identify efficient and allele-specific siRNA. Using a psiCHECK dual luciferase vector, we cloned part of the 3'-UTR of *LMNB1* downstream to the *hRluc* gene (green rectangle) used as reference. The *hLuc* gene (*Renilla*, yellow rectangle) in the plasmid is used to normalize the transfection efficiency (T7 and HSV-TK indicate promoter types). Two vectors were generated, one with the 'T' and one with the 'C' allele at rs1051644. The reporter vector was challenged with each of 19 siRNA containing the rs1051644 'C' or 'T' allele in one of the 19 possible positions (see Supplementary Table 2 for details) at two different concentrations (12.5 nM, **B**; 30 nM, **C**). A scramble siRNA and a siRNA against *hRluc* were used as negative and positive controls, respectively. Ideally, the best siRNA should completely abrogate the matched allele, leaving the unmatched allele unchanged (**A**, bar chart). Results of this screening are reported in **B** and **C**. Numbers on the x-axis indicate the position of the mismatch on the siRNA. CTRL+ indicates a non-allele-specific *LMNB1* siRNA. Statistical significant differences (asterisks) between matched (blue) and unmatched (orange) siRNAs are reported (* $P < 0.05$; ** $P < 0.01$; *** $P < 0.001$; two-tailed, Mann-Whitney). The most efficient and allele-specific siRNAs are circled.

positions 3–5 and 9) significantly reduced *LMNB1* protein compared to scramble siRNA ($P < 0.0001$; Supplementary Table 6). Most interestingly, the reduction mediated by ASP-siRNAs at positions 3–5 restored *LMNB1* protein to physiological values (Fig. 3C, D and Supplementary Table 6).

Furthermore, to evaluate the therapeutic potential in ADLD of the selected ASP-siRNAs, they were evaluated for their ability to abrogate *LMNB1*-overexpression dependent cellular phenotypes, such as nuclear blebs (Ferrera *et al.*, 2014; Giorgio *et al.*, 2015) and transcriptome alterations (Bartoletti-Stella *et al.*, 2015) in patient fibroblasts. These experiments were performed after incubation for 120 h, confirming the ability of ASP-siRNAs to restore physiological *LMNB1* expression level at this time point (Supplementary Table 4).

By fluorescent microscopy, we blindly evaluated 5391 nuclei and scored them as regular (oval/spherical) or misshaped (irregular profile, blebs and invaginations). We detected ~10% of nuclear abnormalities in healthy controls and ~40% in patients ($P < 0.0001$; Fig. 4A scramble and Supplementary Table 7). ASP silencing reduced the percentage of misshaped nuclei in ADLD fibroblasts to close to that of wild-type (Fig. 4A–D and Supplementary Table 7).

To evaluate transcriptome alterations, we assessed the ability of the ASP-siRNAs to modulate *RAVER2* and *LRRC15* mRNAs, which are overexpressed in patients with ADLD (Bartoletti-Stella *et al.*, 2015). Cells treated with ASP-siRNAs showed a statistically significant reduction of *RAVER2* (Fig. 4E and Supplementary Table 7; $P < 0.005$) and *LRRC15* expression (Fig. 4F and Supplementary Table 7; $P < 0.005$).

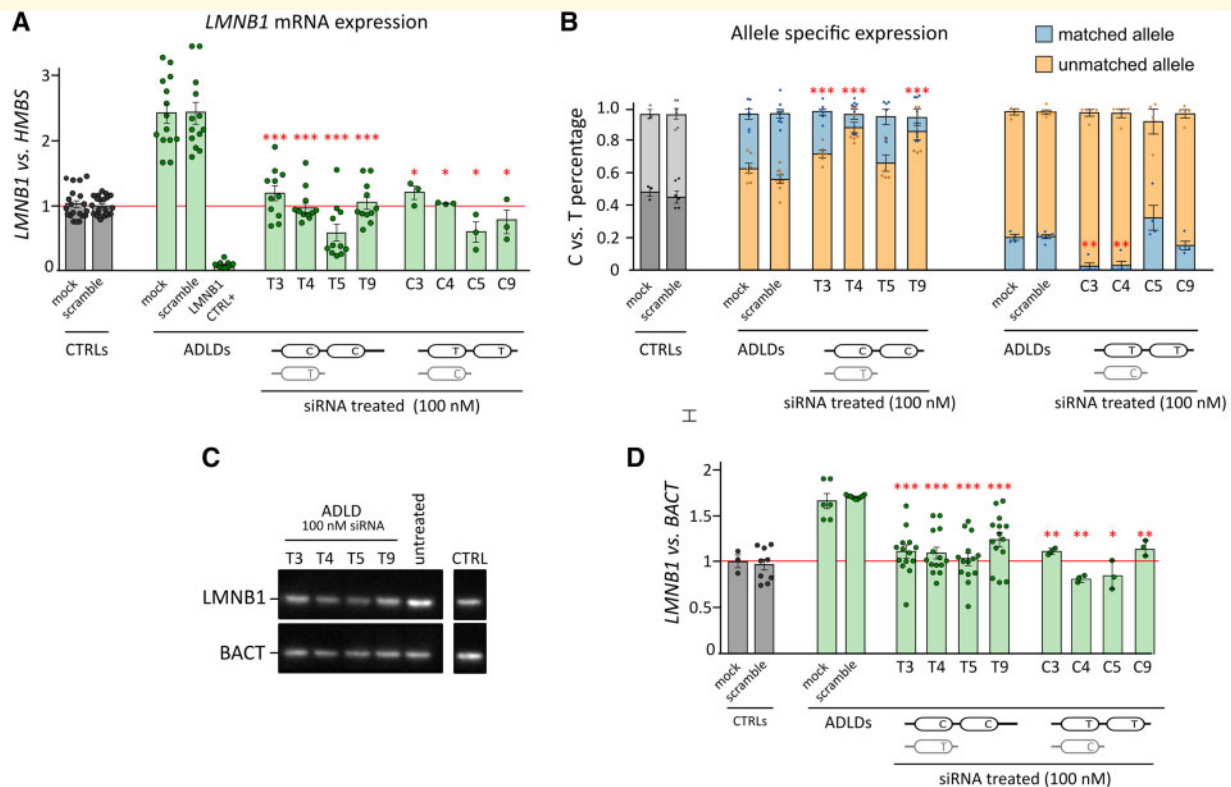


Figure 3 Primary readouts of ASP-siRNA efficacy. ADLD fibroblasts with the ‘C’ allele on the duplicated *LMNB1* copy were treated with 100 nM ASP-siRNAs against the ‘T’ allele of rs1051644 and vice versa for 48 h; mock = untreated cells. Four different ADLD cell lines and three age-matched controls were tested. At least three independent technical replicas were performed. **(A)** Evaluation of total *LMNB1* mRNA levels by quantitative RT-PCR (*LMNB1* versus *HMBS*). Fold-change and SEM (bars) are reported. Statistical significance is given comparing ADLD versus scramble (* $P < 0.05$; ** $P < 0.01$; *** $P < 0.001$; two-tailed, Mann-Whitney). **(B)** Evaluation of allele-specific expression using primer extension assay (allele C versus allele T, percentage). Mean \pm SEM (bars) are reported. Statistical significant values were evaluated comparing ADLD versus scramble (** $P < 0.01$; *** $P < 0.001$; two-tailed, Mann-Whitney). **(C and D)** Evaluation of total *LMNB1* protein by western blot (*LMNB1* versus β -actin). Immunostaining with anti-*LMNB1* and anti- β -actin antibodies are shown as exemplification of the analysis in **C**. Full-length blot is available in the Supplementary material. Fold-change densitometric data and SEM (bars) are shown in **D**. Statistical significant differences (asterisks) are reported for ADLDs versus scramble (* $P < 0.05$; ** $P < 0.01$; *** $P < 0.001$; two-tailed, Mann-Whitney). For **A**, **B**, and **D** the genomic structure of ADLD patients used in the experiments in reference to rs1051644 is shown below.

ASP-siRNA treatment ameliorated ADLD-specific cellular phenotypes in disease-relevant cellular models

Disease-relevant cellular and animal models are essential to study disease progression and to screen potential therapies. To this aim, we validated the ASP-RNAi strategy as an ADLD therapy into directly-reprogrammed ADLD neurons and rat oligodendrocyte cultures overexpressing hLMNB1.

Validation of the therapeutic potential of ASP-siRNA in reprogrammed ADLD neurons

Fibroblasts from three patients with ADLD and three healthy subjects were directly reprogrammed into neurons. About 60% of cells (58% in controls and 64% in patients-derived cells) were effectively reprogrammed as shown by β -III tubulin-positive staining (Supplementary Fig. 1A). As expected, ADLD neurons showed increased *LMNB1* protein levels

compared to control neurons ($P < 0.0001$), an increased number of nuclear abnormalities ($P = 0.0034$) and neurite outgrowth ($P < 0.0001$) (Supplementary Fig. 1E).

To validate our ASP-RNAi strategy, neurons were transduced at two different time points (reprogramming Days 0 and 13) with lentiviral particles (LV-shLMNB1 or LV-scramble shRNA) at a MOI of 50 or 80. Untreated (mock) or treated with LV-scramble shRNA (scramble) ADLD neurons showed an increased *LMNB1* protein level compared to controls (mock $P = 0.0003$; scramble $P < 0.0001$) (Fig. 5A, B and Supplementary Table 8). Notably, neuron transduction with scramble particles does not influence *LMNB1* protein levels compared to non-infected cells ($P = 0.8696$) (Fig. 5A, B and Supplementary Table 8). The treatment at Day 0 with the allele-specific shRNA-T4 (shLMNB1 d0) reduces *LMNB1* protein of $\sim 30\%$ in ADLD neurons compared to scramble shRNA ($P < 0.0001$), ameliorates ADLD-specific neuronal phenotypes such as nuclear anomalies ($P < 0.0001$) and

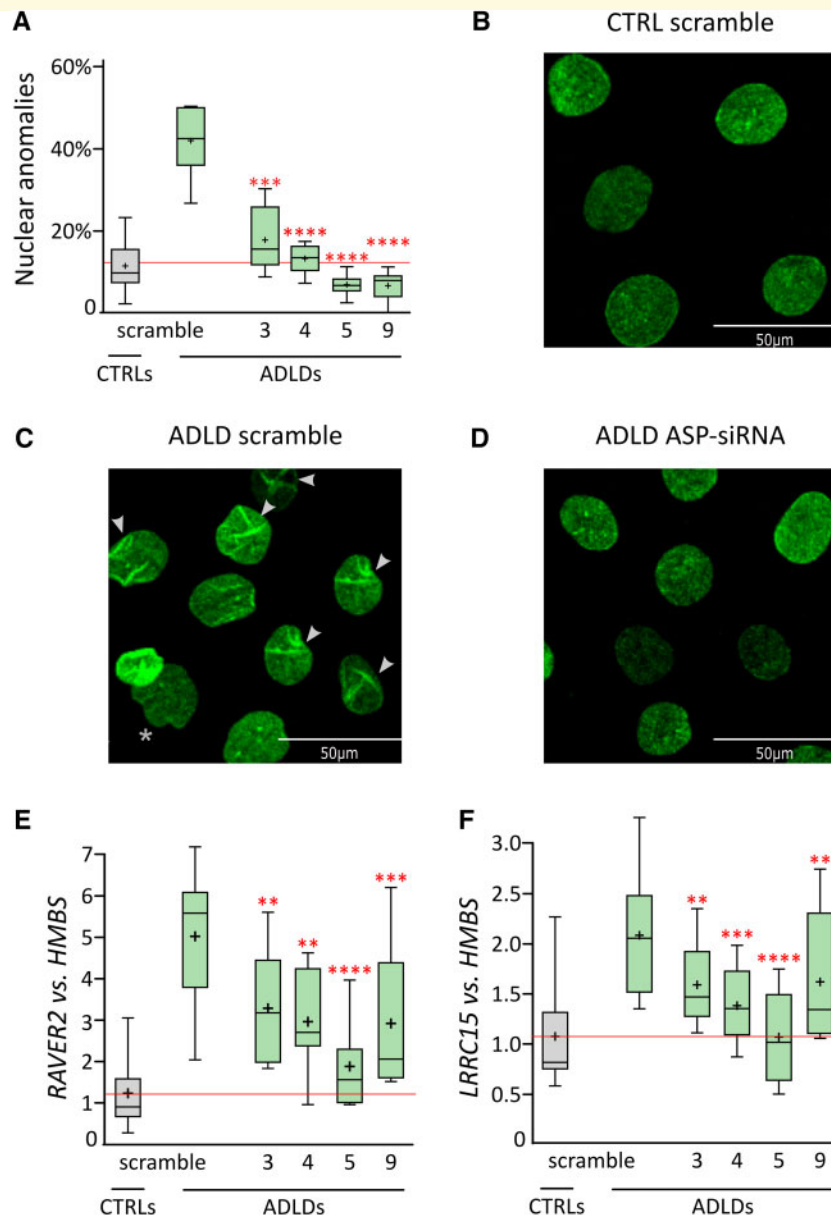


Figure 4 Secondary readouts of ASP-siRNA efficacy. ADLD fibroblasts with the ‘C’ allele on the duplicated *LMNB1* copy were treated with 100 nM ASP-siRNAs against the ‘T’ allele of the SNP and vice versa for 120 h. Four different ADLD cell lines and three age-matched controls were tested. At least three independent experiments were performed. Nuclear shape anomalies were evaluated by fluorescent microscopy after LMNB1 staining. A total of 5391 nuclei were evaluated blind. Fold-change and SEM (bars) are shown in **A**. Statistical significant values show differences between ADLD and scramble (**P < 0.001; ***P < 0.0001; two-tailed, Mann-Whitney). Nuclei from a control line treated with scramble siRNA (CTRL scramble, **B**) and an ADLD line treated with scramble siRNA (ADLD scramble, **C**) or with ASP-siRNAs (ADLD ASP-siRNA, **D**) are shown as exemplification of the analysis. Blebs (asterisk) and invaginations (arrowheads) are highlighted. (**E** and **F**) Box and whisker show quantitative real-time PCR results for *RAVER2* mRNA levels (**E**; *RAVER2* versus *HMBS*) and *LRRC15* (**F**; *LRRC15* versus *HMBS*). Fold-change and SEM (bars) are reported. Statistical significant differences (asterisks) are given for ADLDs versus scramble (**P < 0.02; ***P < 0.001; ****P < 0.0001; two-tailed, Mann-Whitney). In the box and whisker plots, the ends of the box are the upper and lower quartiles; the median is marked by a horizontal line inside the box, while mean is represented by a cross. The highest and lowest observations are represented by two lines extending outside the box.

neurite growth ($P < 0.0001$) (Fig. 5C, D and Supplementary Table 8). On the other hand, the treatment at Day 13 (shLMNB1 d13) induces a minor but significant reduction of LMNB1 levels ($P = 0.0316$) and partly improves the cellular phenotypes (crumpled nuclei; $P = 0.0100$) (Fig. 5A–D and Supplementary Table 8).

Validation of the therapeutic potential of ASP-siRNA in rat oligodendrocyte cultures overexpressing hLMNB1

Primary OPCs were transduced with lentiviral particles (shLMNB1) at a MOI of 50. Five days later, OPCs were transfected with GFP-tagged human LMNB1 expression

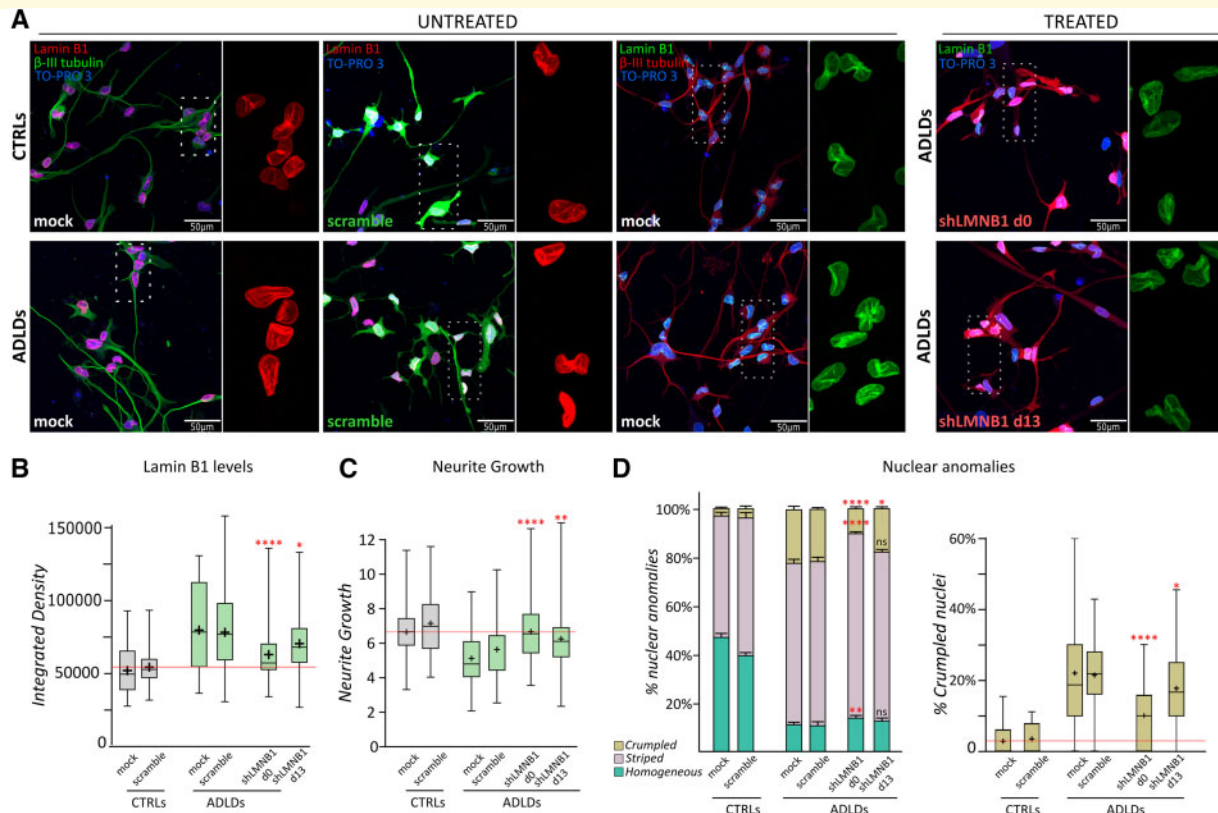


Figure 5 Validation of ASP-RNAi in reprogrammed neurons. (A) Neurons directly reprogrammed from fibroblasts of ADLD patients (ADLDs) or healthy subjects (CTRLs), stained for β -III tubulin. Neurons were cultured with no treatments (mock), or transduced with either scramble lentiviral particles (scramble) or with shLMNB1 viruses at two different time points, reprogramming Day 0 or Day 13 (shLMNB1 d0; shLMNB1 d13). For each panel a 2-fold magnified inset is shown. Note that labelling for LMNB1 protein is presented in green or red, in accordance with the corresponding fluorescent reporter encoded by the infecting viral particles. (B–D) Quantifications of LMNB1 protein levels (B), neurite growth (C) and nuclear anomalies (D) in cells untreated (mock), infected with LV-scramble shRNA (scramble) or with the ASP-vector at Day 0 (shLMNB1 d0) or Day 13 (shLMNB1 d13). Examples of nuclei corresponding to the categories represented in D are shown in Supplementary Fig. 1 (E). Statistically significant differences (asterisks) are shown for comparisons between ADLDs shLMNB1 versus ADLD scramble (B: Mann-Whitney *t*-test; *****P* < 0.0001, **P* = 0.0316; C: Mann-Whitney *t*-test; *****P* < 0.0001, ***P* = 0.0030; D: Mann-Whitney *t*-test; Day 0, crumpled nuclei, *****P* < 0.0001; Day 0 striped nuclei, ***P* = 0.0046; Day 13 crumpled nuclei, **P* = 0.0100; ns, *P* > 0.05). Details of statistical analysis for all comparisons are reported in Supplementary Table 8. Error bars = SEM. Staining: LMNB1 (green or red), β -III tubulin (green or red), LV-scramble (green), ASP-vector (red), cell nuclei/TO-PRO-3 (blue). Scale bars are shown.

plasmids containing the ‘T’ allele (matched allele) or the ‘C’ allele (non-matched allele) of the target SNP (*hLMNB1-T* and *hLMNB1-C*, respectively). When transfected with the GFP-tagged human LMNB1, OPCs (GFP positive, GFP+) consistently showed increased LMNB1 protein level, as detected with immunostaining, compared to non-transfected cells (GFP negative, GFP–, mock) (*P* = 0.0177; Supplementary Fig. 2B and C), and presented nuclear abnormalities [Supplementary Fig. 2D(I–IV)]. Namely, nuclei of GFP+ OPCs showed a unique striped or shrunk pattern suggestive of ongoing nuclear fragmentation [Supplementary Fig. 2D(III and IV)]. This feature occurred with a frequency of ~5% in OPCs overexpressing human LMNB1 while it was virtually absent in GFP– cells [Supplementary Fig. 2D(I and II)]. These data corroborated our oligodendrocyte culture as an appropriate ADLD-relevant cellular model.

OPCs overexpressing the *hLMNB1-T* allele and treated with the allele-specific shRNA-T4 (shLMNB1; matched siRNA) showed a strong reduction of LMNB1 protein levels (*P* < 0.0001) (Fig. 6 and Supplementary Table 9). Interestingly, OPCs overexpressing the *hLMNB1-C* allele (non-matched allele) and treated with the LV-shASP-T4 did not show any difference compared to scramble (*P* = 0.1960) (Fig. 6 and Supplementary Table 9), substantiating the allele specificity of our therapeutic molecule. Finally, ADLD-specific nuclear anomalies (Supplementary Fig. 2) appear to be reduced to about one-third when the ‘T’ allele was silenced while they were essentially maintained in cells overexpressing the ‘C’ allele. We obtained comparable results evaluating LMNB1 levels by both immunostaining and fluorescence of the GFP reporter encoded by the transfected plasmid (Fig. 6 and Supplementary Table 9).

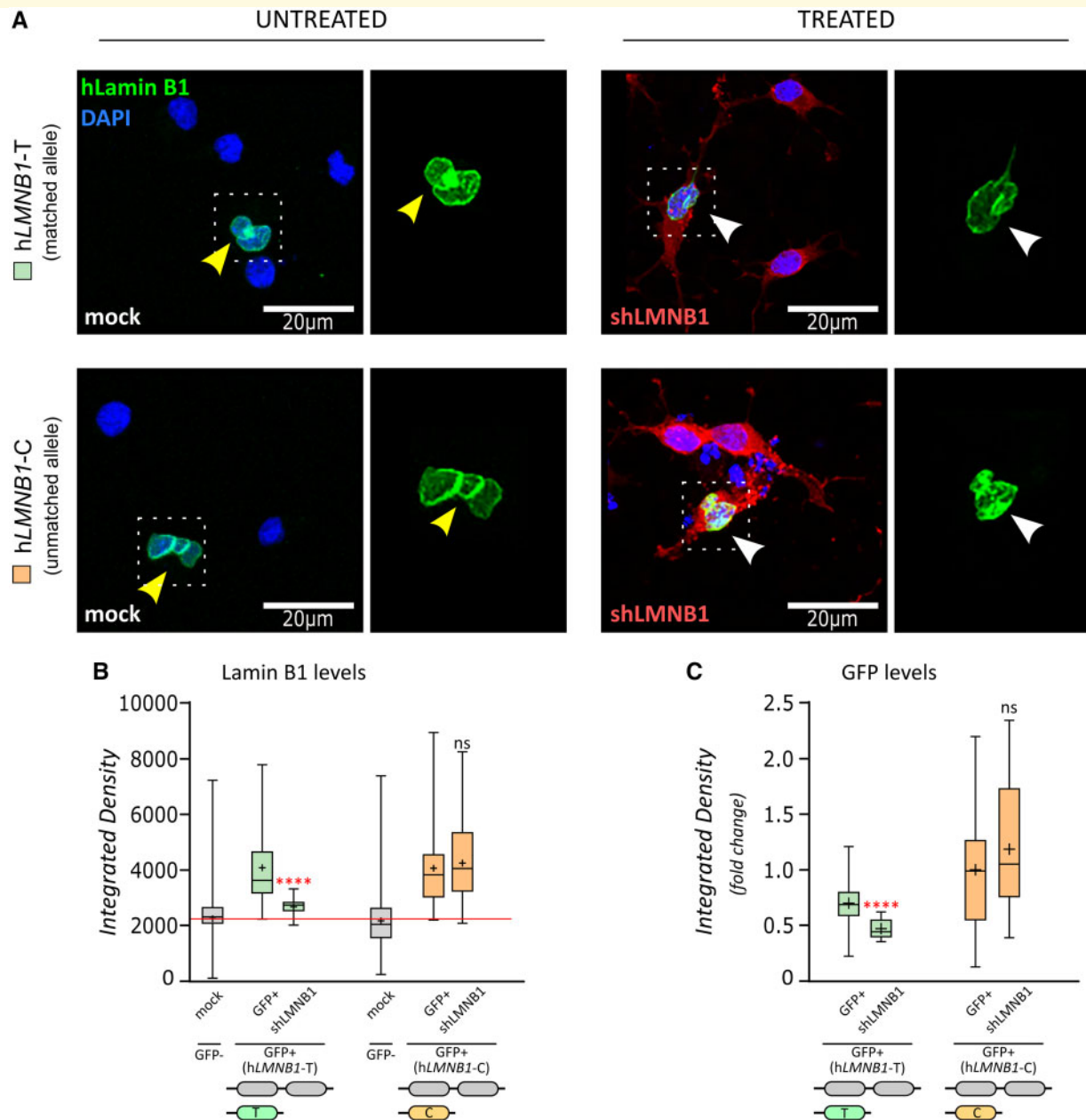


Figure 6 Validation of ASP-RNAi in OPCs overexpressing hLMNB1. (A) OPCs transfected to overexpress the 'T' (hLMNB1-T; top) or the 'C' (hLMNB1-C; bottom) allele of the GFP-tagged human LMNB1 (yellow arrows). The human GFP-tagged LMNB1 protein (green) localizes to the cell nuclei (DAPI staining, blue), as expected. Cells were cultured with no treatments (mock; untreated: left) or transduced with the ASP-vector (shLMNB1; treated: right). White arrows indicate effectively transfected (GFP+, green) and transduced (red) cells. For each panel a $\times 2$ magnified inset displaying GFP-tagged LMNB1 is shown. Staining: hLMNB1-GFP protein (green), cells transduced with LV-shLMNB1 (shLMNB1, red), nuclei (DAPI, blue). Scale bars are shown. (B) Quantifications of total LMNB1 protein levels obtained by analyses of human and mouse LMNB1 immunostaining in cells untreated (GFP-; mock), transfected with the GFP-tagged human LMNB1 'T' allele (GFP+ hLMNB1-T) or the GFP-tagged human LMNB1 'C' allele (GFP+ hLMNB1-C), or transfected and treated with the LV-shLMNB1 (shLMNB1). (C) Quantifications of human LMNB1 protein levels based on tagged GFP fluorescence in cells transfected with the GFP-tagged human LMNB1 'T' allele (GFP+ hLMNB1-T) or the GFP-tagged human LMNB1 'C' allele (GFP+ hLMNB1-C) or transfected (GFP+) and infected with the LV-shLMNB1 (shLMNB1). Statistically significant differences are shown for GFP+ shLMNB1 versus GFP+ or GFP- cells (Mann-Whitney *t*-test; *****P* < 0.0001; ns, *P* > 0.05).

Discussion

ADLD is a fatal neurological disorder for which no treatment is available. Because the age of onset is usually

beyond 35 years of age, this disease represents an ideal candidate for a treatment that could be administered in the pre-symptomatic phase. The brain and spinal cord MRI findings can precede clinical manifestations by years,

thus monitoring patients may allow starting the treatment when the first MRI signs occur (Nahhas, 2016).

As ADLD is caused primarily by *LMNB1* gene duplication-mediated overexpression, the treatment of choice would be a drug capable of reducing its expression. On the other hand, excessive gene knockdown may have deleterious effects, as shown in cellular and mouse models (Liu *et al.*, 2000; Harborth *et al.*, 2001; Vergnes *et al.*, 2004; Ji *et al.*, 2007; Coffinier *et al.*, 2010; Bartoletti-Stella *et al.*, 2015; Giacomini *et al.*, 2016). Given this context, a fine modulation of *LMNB1* expression is required for an effective ADLD therapeutic option.

We reasoned that ASP-RNAi was the best choice, given that it can specifically inhibit the expression of one of the three *LMNB1* alleles in an *LMNB1*-duplicated patient, avoiding a potentially excessive and harmful *LMNB1* knockdown.

ADLD patients have three equally-expressed *LMNB1* alleles that we discriminated by exploiting the rs1051644 SNP. Thus, to restore physiological *LMNB1* levels, we chose to target the non-duplicated allele, maintaining only two transcriptionally active copies of the gene, as in normal subjects.

Identification of efficient and specific ASP-siRNAs required an *in vitro* screening using a dual-reporter vector challenged with a library of all possible 19 siRNAs targeting rs1051644. We found three ASP-siRNAs able to silence the target allele with minimal suppression of the non-target one (positions 3, 4 and 9). In treated ADLD-derived fibroblasts, we proved that *LMNB1* expression and protein levels were restored to normal levels.

Thus, we planned testing the effects of ASP-siRNAs on *LMNB1*-connected biological changes. Lamins are essential building blocks of the nuclear lamina and mechanically enforce the nuclear morphology (de Leeuw *et al.*, 2018). Generally, disease-causing mutant lamins lead to abnormal nuclear morphology that is visible on the cellular level. In lamin knockout experiments, cells appear to have small fragile nuclei, decreased nuclear stiffness and nuclear shape can be affected (Vergnes *et al.*, 2004; Lammerding *et al.*, 2006; Coffinier *et al.*, 2011; Shimi *et al.*, 2011). Lamin overexpression causes blebs and invaginations of the nuclear envelope (Prufert *et al.*, 2004; Friedl *et al.*, 2011) and increases nuclear stiffness (Ferrera *et al.*, 2014). Following our treatment with ASP-siRNAs, we showed that ADLD fibroblasts quickly reverted to the nuclear shape of regular nuclei.

Beyond their structural role, a fraction of lamins also reside throughout the nuclear interior where they have important roles in essential cellular processes such as transcription, DNA replication, cell cycle progression, and chromatin organization (Dechat *et al.*, 2010; Buchwalter *et al.*, 2019). We demonstrated that the expression of two known genes affected by *LMNB1* levels, *RAVER2* and *LRRC15*, significantly decreased after treatment. Corroborating the clinical relevance of ASP-siRNAs, we previously reported that *RAVER2* is directly involved in

ADLD pathogenesis: its overexpression results in abnormal splicing patterns of several phosphotyrosine binding domain (PTB)-target genes and of proteolipid protein 1 (PLP1), the predominant protein component of myelin (Bartoletti-Stella *et al.*, 2015), demonstrated previously to be implicated in ADLD (Heng *et al.*, 2013).

Overall, our results pinpoint two ASP-siRNAs (positions 3 and 4) able to silence specifically one of the three *LMNB1* alleles in ADLD cells, restoring physiological levels of mRNA and protein and ameliorating disease-relevant cellular phenotypes in patients' fibroblasts.

To demonstrate ASP-silencing efficacy in cell types more relevant to ADLD, we generated two cellular models: (i) neurons directly reprogrammed from human fibroblasts; and (ii) rat OPCs overexpressing human *LMNB1*. We proved that both cellular models presented increased *LMNB1* levels compared to control cells and showed ADLD-specific cellular phenotypes, supporting their relevance as *in vitro* preclinical tools.

Both cellular models were treated with the most efficient ASP-molecule (LV-ASP-T4 shRNA).

The treatment reduced *LMNB1* protein level in both models and ameliorated ADLD-specific cellular abnormalities, validating the therapeutic potential of our RNA molecule. Furthermore, rat OPCs overexpressing human *LMNB1* allowed us to further assess the allele specificity of our strategy. Indeed, the LV-ASP-T4 shRNA effectively silenced only cells overexpressing the human *LMNB1* allele carrying the 'T' allele of the targeted rs1051644 SNP (matched allele).

ADLD is a late-onset disease with a 30-year long preclinical phase. We think it would be more effective to treat patients in this pre-symptomatic window to prevent *LMNB1* overexpression-dependent cellular degeneration in brain. To prove our hypothesis, neurons were treated at two different time points. As expected, treating cells at the start of the reprogramming process (Day 0) showed a significant improvement of ADLD-specific neuronal phenotypes, compared to the treatment performed at reprogramming Day 13 (d13), which only partially ameliorates cellular phenotypes.

Following these results, at least one RNA molecule (ASP-T4) is approved for a further step of validation, i.e. *in vivo* treatment of animal models. Our ASP-silencing strategy requires a fully humanized mouse carrying three human *LMNB1* alleles, recapitulating ADLD phenotypes and heterozygous for the SNP targeted by ASP-siRNAs (rs1051644). This mouse model would mimic the precise genomic context of *LMNB1* duplication found in patients and would allow the *in vivo* evaluation of efficacy and selectivity (allele specificity) of the identified siRNAs. Unfortunately, both the two mouse models currently available (*Lmnb1*^{BAC} and *PLP-LMNB1*^{Tg}) (Heng *et al.*, 2013; Rolyan *et al.*, 2015) are not suitable for this experiment. The *Lmnb1*^{BAC} mice overexpress a murine multiple *Lmnb1* transgene, not targetable by our ASP-siRNA strategy. In the *PLP-LMNB1*^{Tg} mouse, the human overexpressed *LMNB1*

Table 1 Genetic diseases associated with gene(s) duplication treatable by ASP-siRNA

Disease	OMIM	Locus	Target gene
Single gene disorders			
Parkinson's disease	168600	4q21	SNCA
ADLD	169500	5q35	LMNB1
Charcot-Marie-Tooth type 1	118220	17p12	PMP22
Alzheimer's disease	104300	21q21.3	APP
Pelizaeus-Merzbacher disease	312080	Xq22.2	PLP1
Rett syndrome	300260	Xq28	MECP2
Genomic disorders			
Microduplication 7q11.23	609757	7q11.23	ELN, GTF2I?
Spinocerebellar ataxia type 20	608687	11q12	DAGLA?
Microduplication 15q11-q13	608636	15q11.2-q13.1	GABRA5?, GABRB3?, UBE3A
Potocki-Lupski syndrome	610883	17p11.2	RAI1
Microduplication 17p13.3	613215	17p13.3	LIS1, YWAHAE
Microduplication 22q11.2	608363	22q11.2	TXNRD2, COMT, ARVCF?
Microduplication Xp11.22	300706	Xp11.22	HUWE1

Question marks indicate proposed causative genes.

gene does not contain the 3'-UTR, to which the rs1051644 maps.

To overcome this obstacle, we are working to generate a chimeric mouse model in which oligodendroglial cells and myelin will be patient-derived, by performing multifocal neonatal engraftment in immunocompromised dysmyelinated mice (*shiverer* mice) with OPCs derived from patients' hiPSCs, as already described (Wang *et al.*, 2013; Osipovitch *et al.*, 2019). This mouse model would represent a unique system to evaluate the *in vivo* preclinical efficacy of ASP-siRNAs in ADLD.

Delivery of ASP-siRNAs to their target tissue and cellular internalization are still major challenges that limit their full use in therapy. Recently, clinically relevant delivery of siRNAs has been achieved exploiting two main classes of vehicles: non-viral (e.g. liposomes, exosomes, polymeric nanoparticles) or viral vectors (herpes simplex virus type 1, adenovirus, adeno-associated virus and lentivirus) (van den Boorn *et al.*, 2011; Choudhury *et al.*, 2016; Mishra *et al.*, 2017). Among the latter, adeno-associated type 9 (AAV-9) viruses show an efficient tropism for brain cells both *in vitro* and *in vivo*, including neurons, oligodendrocytes and glial cells (Foust *et al.*, 2009; Aschauer *et al.*, 2013; Bucher *et al.*, 2014; Dufour *et al.*, 2014). Moreover, AAV-9 viruses pass the blood-brain barrier, present a low risk of insertional mutagenesis and trigger diminished immune responses (Foust *et al.*, 2009; Aschauer *et al.*, 2013; Dufour *et al.*, 2014; Gong *et al.*, 2015; Saraiva *et al.*, 2016). AAV-9 viruses have been used in different clinical trials, and are thus an interesting delivery system for ASP-siRNA in ADLD (Foust *et al.*, 2009; Aschauer *et al.*, 2013; Dufour *et al.*, 2014; Gong *et al.*, 2015; Saraiva *et al.*, 2016). Of note, several reports showed that nanoparticle-linked siRNA can be delivered *in vivo* into the brain by intranasal administration to knock down target proteins into neurons, microglia and

astrocytes, opening new routes of administration distinct from the more invasive intrathecal injection-mediated delivery strategy (Mistry *et al.*, 2009; Biddlestone-Thorpe *et al.*, 2012; Rodriguez *et al.*, 2017).

Our work represents a proof-of-concept for the use of ASP-RNAi in genetic disorders associated with gene(s) duplication, and could be applied to rare conditions such as Pelizaeus-Merzbacher disease, Charcot-Marie-Tooth type 1A and Rett syndrome (Table 1). Aside from single-gene diseases, disorders associated with large genomic copy number gains might be potentially treated by ASP-siRNA whenever the pathological phenotype is associated to the overexpression of different dosage-sensitive genes, requiring a multiple-target ASP-siRNA strategy.

Overall, our work demonstrated that ASP-silencing is a suitable and promising therapeutic option for ADLD, prompting further *in vivo* studies to validate our results before clinical trials. Moreover, our results have a broad translational value extending to several pathological conditions linked to gene copy number variations.

Acknowledgements

We thank Dr Malin Parmar at the University of Lund (Sweden) for providing plasmid vectors used in fibroblasts-to-neuron reprogramming. We are also indebted to the ADLD family members who participated in this study. Patent approved for the ASP-siRNA sequences n. 102017000121288 entitled 'RNA interference mediated therapy for neurodegenerative diseases'.

Funding

The work was supported by the Fondazione Umberto Veronesi (post-doctoral fellowship 2017 to EG), Ricerca

locale MURST ex 60%, the ‘Associazione E. E. Rulfo per la ricerca biomedica’ to A.Br. Ricerca locale MURST ex 60% to A.Bu; Marie Curie Individual Fellowship to P.R.d.V.C. (DISMOD-HD); Ministero dell’Istruzione, dell’Università e della Ricerca – MIUR ‘Dipartimenti di Eccellenza 2018–2022’ to Department of Medical Sciences (Project D15D18000410001) to A.Br. and Department of Neuroscience Rita Levi Montalcini to A.Bu. COST Action CA17103: Delivery of Antisense RNA Therapeutics.

Competing interests

A.Br. and E.G. are authors of the patent n. 102017000121288, concerning the ASP-siRNA sequences.

Supplementary material

Supplementary material is available at *Brain* online.

References

- Allen EH, Atkinson SD, Liao H, Moore JE, Leslie Pedrioli DM, Smith FJ, et al. Allele-specific siRNA silencing for the common keratin 12 founder mutation in Meesmann epithelial corneal dystrophy. *Investig Ophthalmol Vis Sci* 2013; 54: 494–502.
- Alves S, Nascimento-Ferreira I, Auregan G, Hassig R, Dufour N, Brouillet E, et al. Allele-specific RNA silencing of mutant ataxin-3 mediates neuroprotection in a rat model of Machado-Joseph disease. *PLoS One* 2008; 3: e3341.
- Antonarakis SE. Down syndrome and the complexity of genome dosage imbalance. *Nat Rev Genet* 2017; 18: 147–63.
- Aschauer DF, Kreuz S, Rumpel S. Analysis of transduction efficiency, tropism and axonal transport of AAV serotypes 1, 2, 5, 6, 8 and 9 in the mouse brain. *PLoS One* 2013; 8: e76310.
- Bartoletti-Stella A, Gasparini L, Giacomini C, Corrado P, Terlizzi R, Giorgio E, et al. Messenger RNA processing is altered in autosomal dominant leukodystrophy. *Hum Mol Genet* 2015; 24: 2746–56.
- Biddlestone-Thorpe L, Marchi N, Guo K, Ghosh C, Janigro D, Valerie K, et al. Nanomaterial-mediated CNS delivery of diagnostic and therapeutic agents. *Adv Drug Del Rev* 2012; 64: 605–13.
- Boda E, Di Maria S, Rosa P, Taylor V, Abbracchio MP, Buffo A. Early phenotypic asymmetry of sister oligodendrocyte progenitor cells after mitosis and its modulation by aging and extrinsic factors. *Glia* 2015; 63: 271–86.
- Bucher T, Dubreil L, Colle MA, Maquigneau M, Deniaud J, Ledevin M, et al. Intracisternal delivery of AAV9 results in oligodendrocyte and motor neuron transduction in the whole central nervous system of cats. *Gene Ther* 2014; 21: 522–8.
- Buchwalter A, Kaneshiro JM, Hetzer MW. Coaching from the sidelines: the nuclear periphery in genome regulation. *Nat Rev Genet* 2019; 20: 39–50.
- Bumcrot D, Manoharan M, Kotliansky V, Sah DW. RNAi therapeutics: a potential new class of pharmaceutical drugs. *Nat Chem Biol* 2006; 2: 711–9.
- Camps J, Wangsa D, Falke M, Brown M, Case CM, Erdos MR, et al. Loss of lamin B1 results in prolongation of S phase and decondensation of chromosome territories. *FASEB J* 2014; 28: 3423–34.
- Choudhury SR, Fitzpatrick Z, Harris AF, Maitland SA, Ferreira JS, Zhang Y, et al. In vivo selection yields AAV-B1 capsid for central nervous system and muscle gene therapy. *Mol Ther* 2016; 24: 1247–57.
- Coelho T, Adams D, Silva A, Lozeron P, Hawkins PN, Mant T, et al. Safety and efficacy of RNAi therapy for transthyretin amyloidosis. *N Engl J Med* 2013; 369: 819–29.
- Coffeen CM, McKenna CE, Koeppen AH, Plaster NM, Maragakis N, Mihalopoulos J, et al. Genetic localization of an autosomal dominant leukodystrophy mimicking chronic progressive multiple sclerosis to chromosome 5q31. *Hum Mol Genet* 2000; 9: 787–93.
- Coffinier C, Chang SY, Nobumori C, Tu Y, Farber EA, Toth JI, et al. Abnormal development of the cerebral cortex and cerebellum in the setting of lamin B2 deficiency. *Proc Natl Acad Sci USA* 2010; 107: 5076–81.
- Coffinier C, Jung HJ, Nobumori C, Chang S, Tu Y, Barnes RH 2nd, et al. Deficiencies in lamin B1 and lamin B2 cause neurodevelopmental defects and distinct nuclear shape abnormalities in neurons. *Mol Biol Cell* 2011; 22: 4683–93.
- Davis ME, Zuckerman JE, Choi CH, Seligson D, Tolcher A, Alabi CA, et al. Evidence of RNAi in humans from systemically administered siRNA via targeted nanoparticles. *Nature* 2010; 464: 1067–70.
- de Fougerolles A, Vornlocher HP, Maraganore J, Lieberman J. Interfering with disease: a progress report on siRNA-based therapeutics. *Nat Rev Drug Discov* 2007; 6: 443–53.
- de Leeuw R, Gruenbaum Y, Medalia O. Nuclear lamins: thin filaments with major functions. *Trends Cell Biol* 2018; 28: 34–45.
- Dechat T, Gesson K, Foisner R. Lamina-independent lamins in the nuclear interior serve important functions. *Cold Spring Harb Symp Quant Biol* 2010; 75: 533–43.
- Deshpande A, Weiss LA. Recurrent reciprocal copy number variants: roles and rules in neurodevelopmental disorders. *Dev Neurobiol* 2018; 78: 519–30.
- DeVincenzo J, Lambkin-Williams R, Wilkinson T, Cehelsky J, Nochur S, Walsh E, et al. A randomized, double-blind, placebo-controlled study of an RNAi-based therapy directed against respiratory syncytial virus. *Proc Natl Acad Sci USA* 2010; 107: 8800–5.
- Drouin-Ouellet J, Lau S, Brattas PL, Rylander Ottosson D, Pirces K, Grassi DA, et al. REST suppression mediates neural conversion of adult human fibroblasts via microRNA-dependent and -independent pathways. *EMBO Mol Med* 2017a; 9: 1117–31.
- Drouin-Ouellet J, Pirces K, Barker RA, Jakobsson J, Parmar M. Direct neuronal reprogramming for disease modeling studies using patient-derived neurons: what have we learned? *Front Neurosci* 2017b; 11: 530.
- Dufour BD, Smith CA, Clark RL, Walker TR, McBride JL. Intrajugular vein delivery of AAV9-RNAi prevents neuropathological changes and weight loss in Huntington’s disease mice. *Mol Ther* 2014; 22: 797–810.
- Dyxhoorn DM, Lieberman J. Knocking down disease with siRNAs. *Cell* 2006; 126: 231–5.
- Eldridge R, Anayiotos CP, Schlesinger S, Cowen D, Bever C, Patronas N, et al. Hereditary adult-onset leukodystrophy simulating chronic progressive multiple sclerosis. *N Engl J Med* 1984; 311: 948–53.
- Ferrera D, Canale C, Marotta R, Mazzaro N, Gritti M, Mazzanti M, et al. Lamin B1 overexpression increases nuclear rigidity in autosomal dominant leukodystrophy fibroblasts. *FASEB J* 2014; 28(9): 3906–18.
- Foust KD, Nurre E, Montgomery CL, Hernandez A, Chan CM, Kaspar BK. Intravascular AAV9 preferentially targets neonatal neurons and adult astrocytes. *Nat Biotechnol* 2009; 27: 59–65.
- Friedl P, Wolf K, Lammerding J. Nuclear mechanics during cell migration. *Current opinion in cell biology* 2011; 23: 55–64.
- Giacomini C, Mahajani S, Ruffilli R, Marotta R, Gasparini L. Lamin B1 protein is required for dendrite development in primary mouse cortical neurons. *Mol Biol Cell* 2016; 27: 35–47.
- Giorgio E, Robyr D, Spielmann M, Ferrero E, Di Gregorio E, Imperiale D, et al. A large genomic deletion leads to enhancer adoption by the lamin B1 gene: a second path to autosomal dominant adult-onset demyelinating leukodystrophy (ADLD). *Hum Mol Genet* 2015; 24: 3143–54.

- Giorgio E, Rolyan H, Kropp L, Chakka AB, Yatsenko S, Gregorio ED, et al. Analysis of LMNB1 duplications in autosomal dominant leukodystrophy provides insights into duplication mechanisms and allele-specific expression. *Hum Mutat* 2013; 34: 1160–71.
- Gong Y, Mu D, Prabhakar S, Moser A, Musolino P, Ren J, et al. Adenoassociated virus serotype 9-mediated gene therapy for x-linked adrenoleukodystrophy. *Mol Ther* 2015; 23: 824–34.
- Guelen L, Pagie L, Brassat E, Meuleman W, Faza MB, Talhout W, et al. Domain organization of human chromosomes revealed by mapping of nuclear lamina interactions. *Nature* 2008; 453: 948–51.
- Harborth J, Elbashir SM, Bechtel K, Tuschl T, Weber K. Identification of essential genes in cultured mammalian cells using small interfering RNAs. *J Cell Sci* 2001; 114 (Pt 24): 4557–65.
- Haussecker D. The business of RNAi therapeutics. *Hum Gene Ther* 2008; 19: 451–62.
- Heng MY, Lin ST, Verret L, Huang Y, Kamiya S, Padiath QS, et al. Lamin B1 mediates cell-autonomous neuropathology in a leukodystrophy mouse model. *J Clin Invest* 2013; 123: 2719–29.
- Hohjoh H. Disease-causing allele-specific silencing by RNA interference. *Pharmaceuticals* 2013; 6: 522–35.
- Jacquemont S, Reymond A, Zufferey F, Harewood L, Walters RG, Kotalik Z, et al. Mirror extreme BMI phenotypes associated with gene dosage at the chromosome 16p11.2 locus. *Nature* 2011; 478: 97–102.
- Ji JY, Lee RT, Vergnes L, Fong LG, Stewart CL, Reue K, et al. Cell nuclei spin in the absence of lamin b1. *J Biol Chem* 2007; 282: 20015–26.
- Lammerding J, Fong LG, Ji JY, Reue K, Stewart CL, Young SG, et al. Lamins A and C but not lamin B1 regulate nuclear mechanics. *J Biol Chem* 2006; 281: 25768–80.
- Lek M, Karczewski KJ, Minikel EV, Samocha KE, Banks E, Fennell T, et al. Analysis of protein-coding genetic variation in 60,706 humans. *Nature* 2016; 536: 285–91.
- Levin AA. Treating Disease at the RNA Level with Oligonucleotides. *N Engl J Med* 2019; 380: 57–70.
- Liao H, Irvine AD, Macewen CJ, Weed KH, Porter L, Corden LD, et al. Development of allele-specific therapeutic siRNA in Meesmann epithelial corneal dystrophy. *PLoS One* 2011; 6: e28582.
- Lin ST, Fu YH. miR-23 regulation of lamin B1 is crucial for oligodendrocyte development and myelination. *Dis Model Mech* 2009; 2: 178–88.
- Liu J, Rolef Ben-Shahar T, Riemer D, Treinin M, Spann P, Weber K, et al. Essential roles for *Caenorhabditis elegans* lamin gene in nuclear organization, cell cycle progression, and spatial organization of nuclear pore complexes. *Mol Biol Cell* 2000; 11: 3937–47.
- Loy RE, Lueck JD, Mostajo-Radji MA, Carrell EM, Dirksen RT. Allele-specific gene silencing in two mouse models of autosomal dominant skeletal myopathy. *PLoS One* 2012; 7: e49757.
- Miller VM, Gouvion CM, Davidson BL, Paulson HL. Targeting Alzheimer's disease genes with RNA interference: an efficient strategy for silencing mutant alleles. *Nucleic Acids Res* 2004; 32: 661–8.
- Miller VM, Xia H, Marrs GL, Gouvion CM, Lee G, Davidson BL, et al. Allele-specific silencing of dominant disease genes. *Proc Natl Acad Sci USA* 2003; 100: 7195–200.
- Mishra DK, Balekar N, Mishra PK. Nanoengineered strategies for siRNA delivery: from target assessment to cancer therapeutic efficacy. *Drug Deliv Transl Res* 2017; 7: 346–58.
- Mistry A, Stolnik S, Illum L. Nanoparticles for direct nose-to-brain delivery of drugs. *Int J Pharm* 2009; 379: 146–57.
- Nahhas N, Sabet Rasekh P, Vanderver A, Padiath QS. Autosomal Dominant Leukodystrophy with Autonomic Disease. In: Adam MP, Ardinger HH, Pagon RA, Wallace SE, Bean LJH, Mefford HC, Stephens K, Amemiya A, Ledbetter N, editors. *GeneReviews*® [Internet]. Seattle (WA): University of Washington, Seattle; 2016.
- Nguyen T, Menocal EM, Harborth J, Fruehauf JH. RNAi therapeutics: an update on delivery. *Curr Opin Mol Ther* 2008; 10: 158–67.
- Nmezi B, Giorgio E, Raininko R, Lehman A, Spielmann M, Koenig MK, et al. Genomic deletions upstream of lamin B1 lead to atypical autosomal dominant leukodystrophy. *Neurol Genet* 2019; 5: e305.
- Nobrega C, Nascimento-Ferreira I, Onofre I, Albuquerque D, Deglon N, de Almeida LP. RNA interference mitigates motor and neuropathological deficits in a cerebellar mouse model of Machado-Joseph disease. *PLoS One* 2014; 9: e100086.
- Nobrega C, Nascimento-Ferreira I, Onofre I, Albuquerque D, Hirai H, Deglon N, et al. Silencing mutant ataxin-3 rescues motor deficits and neuropathology in Machado-Joseph disease transgenic mice. *PLoS One* 2013; 8: e52396.
- Osipovitch M, Asenjo Martinez A, Mariani JN, Cornwell A, Dhaliwal S, Zou L, et al. Human ESC-derived chimeric mouse models of huntington's disease reveal cell-intrinsic defects in glial progenitor cell differentiation. *Cell Stem Cell* 2019; 24: 107–22.e7.
- Padiath QS, Saigoh K, Schiffmann R, Asahara H, Yamada T, Koeppen A, et al. Lamin B1 duplications cause autosomal dominant leukodystrophy. *Nat Genet* 2006; 38: 1114–23.
- Prufert K, Vogel A, Krohne G. The lamin CxxM motif promotes nuclear membrane growth. *J Cell Sci* 2004; 117 (Pt 25): 6105–16.
- Quattrocchio G, Leombruni S, Vaula G, Bergui M, Riva A, Bradac GB, et al. Autosomal dominant late-onset leukoencephalopathy. Clinical report of a new Italian family. *Eur Neurol* 1997; 37: 53–61.
- Rodriguez M, Kaushik A, Lapierre J, Dever SM, El-Hage N, Nair M. Electro-magnetic nano-particle bound Beclin1 siRNA crosses the blood-brain barrier to attenuate the inflammatory effects of HIV-1 infection in vitro. *J Neuroimmune Pharmacol* 2017; 12: 120–32.
- Rolyan H, Tyurina YY, Hernandez M, Amoscatto AA, Sparvero LJ, Nmezi BC, et al. Defects of lipid synthesis are linked to the age-dependent demyelination caused by Lamin B1 overexpression. *J Neurosci* 2015; 35: 12002–17.
- Saraiva J, Nobre RJ, Pereira de Almeida L. Gene therapy for the CNS using AAVs: the impact of systemic delivery by AAV9. *J Controlled Release* 2016; 241: 94–109.
- Scholefield J, Greenberg LJ, Weinberg MS, Arbutnot PB, Abdelgany A, Wood MJ. Design of RNAi hairpins for mutation-specific silencing of ataxin-7 and correction of a SCA7 phenotype. *PLoS One* 2009; 4: e7232.
- Scholefield J, Watson L, Smith D, Greenberg J, Wood MJ. Allele-specific silencing of mutant Ataxin-7 in SCA7 patient-derived fibroblasts. *Eur J Hum Genet* 2014; 22: 1369–75.
- Schwarz DS, Ding H, Kennington L, Moore JT, Schelter J, Burchard J, et al. Designing siRNA that distinguish between genes that differ by a single nucleotide. *PLoS Genet* 2006; 2: e140.
- Shimi T, Butin-Israeli V, Adam SA, Hamanaka RB, Goldman AE, Lucas CA, et al. The role of nuclear lamin B1 in cell proliferation and senescence. *Genes Dev* 2011; 25: 2579–93.
- Shrigley S, Pirce K, Barker RA, Parmar M, Drouin-Ouellet J. Simple generation of a high yield culture of induced neurons from human adult skin fibroblasts. *J Vis Exp* 2018;132.
- Smith FJ, Hickerson RP, Sayers JM, Reeves RE, Contag CH, Leake D, et al. Development of therapeutic siRNAs for pachyonychia congenita. *The Journal of investigative dermatology* 2008; 128: 50–8.
- Takahashi M, Katagiri T, Furuya H, Hohjoh H. Disease-causing allele-specific silencing against the ALK2 mutants, R206H and G356D, in fibrodysplasia ossificans progressiva. *Gene Ther* 2012; 19: 781–5.
- Takahashi M, Watanabe S, Murata M, Furuya H, Kanazawa I, Wada K, et al. Tailor-made RNAi knockdown against triplet repeat disease-causing alleles. *Proc Natl Acad Sci USA* 2010; 107: 21731–6.
- Tang CW, Maya-Mendoza A, Martin C, Zeng K, Chen S, Feret D, et al. The integrity of a lamin-B1-dependent nucleoskeleton is a fundamental determinant of RNA synthesis in human cells. *J Cell Sci* 2008; 121 (Pt 7): 1014–24.
- van den Boorn JG, Schlee M, Coch C, Hartmann G. siRNA delivery with exosome nanoparticles. *Nat Biotechnol* 2011; 29: 325–6.

- van Paassen BW, van der Kooij AJ, van Spaendonck-Zwarts KY, Verhamme C, Baas F, de Visser M. PMP22 related neuropathies: charcot-marie-tooth disease type 1a and hereditary neuropathy with liability to pressure palsies. *Orphanet J Rare Dis* 2014; 9: 38.
- Vergnes L, Peterfy M, Bergo MO, Young SG, Reue K. Lamin B1 is required for mouse development and nuclear integrity. *Proc Natl Acad Sci USA* 2004; 101: 10428–33.
- Wang S, Bates J, Li X, Schanz S, Chandler-Militello D, Levine C, et al. Human iPSC-derived oligodendrocyte progenitor cells can myelinate and rescue a mouse model of congenital hypomyelination. *Cell Stem Cell* 2013; 12: 252–64.
- Whitehead KA, Langer R, Anderson DG. Knocking down barriers: advances in siRNA delivery. *Nature reviews Drug discovery* 2009; 8: 129–38.